JOURNAL OF Applied Polymer SCIENCE

Preparation, Characterization and the Effect of Carboxymethylated Chitosan-Cellulose Derivatives Hydrogels on Wound Healing

Lihong Fan,[1] Chang Tan,[1] Libo Wang,[1] Xiaoran Pan,[1] Mi Cao,[1] Feng Wen,[1] Weiguo Xie,[2] Min Nie[3]

[1]College of Chemical Engineering, Wuhan University of technology, Wuhan 430070, China

[2]The Third Hospital of Wuhan, Wuhan 430060, China

[3]The State Key Laboratory Breeding Base of Basic Science of Stomatology, Hubei Province & Key Laboratory of Oral Biomedicine (Wuhan University), Wuhan 430079, China

Lihong Fan and Min Nie contributed equally to this work.

Correspondence to: L. Fan (E-mail: lihongfan2000@hotmail.com) or M. Nie (E-mail: nm_min@yahoo.com.cn)

ABSTRACT: Oxidized carboxymethyl cellulose (OCMC) was prepared by an oxidation reaction of carboxymethyl cellulose in the presence of sodium periodate. *In situ* crosslinked hydrogels were obtained through the crosslinking reaction between the active aldehyde of OCMC and the amino groups of the carboxymethyl chitosan (CMCS). The structure of the hydrogels was characterized by FTIR and scanning electron microscopy. Gelation time test showed that the hydrogel had the shortest gelation time of 24 s. The equilibrium fluid content, which represented the swelling degree, was evaluated and we found that the pH increased from 3.0 to 9.0, the equilibrium fluid content increased, and the highest equilibrium fluid content reached 312.83% as pH = 9.0. The wound healing efficacy of the hydrogel was evaluated in experimental deep second degree burns using a rat model. Results indicated that the wound covered with hydrogel was completely filled with new epithelium within 2 weeks, without any significant adverse reactions. The *in situ* crosslinked hydrogel fulfilled many critical elements in a wound dressing material. © 2012 Wiley Periodicals, Inc. J. Appl. Polym. Sci. 000: 000–000, 2012

KEYWORDS: cellulose and other wood products; gels; biomedical applications

Received 25 April 2012; accepted 7 August 2012; published online
DOI: 10.1002/app.38456

INTRODUCTION

Hydrogels consist of three-dimensional hydrophilic polymer networks in which a large amount of water is interposed. Because of their unique properties, a wide range of medical, pharmaceutical, and prosthetic applications have been proposed for them.[1] Due to possessing the features of moist wound healing with good fluid absorbance, hydrogels are transparent to allow the monitoring of healing. *In situ* forming hydrogels that mould into the shape of wound defect will have advantages over the use of preformed hydrogel scaffolds since it would enable conformability of the dressing on wounds without wrinkling or fluting. Most commercially available dressings in the form of membranes and sheets are problematic as far as the conformability is concerned and the *in situ* formed dressings will therefore be superior to preformed dressings. Due to their biodegradable activity, 3D structure, and generating a favorable microenvironment for cell growth and/or differentiation,[2] hydrogels from polysaccharides are particularly attractive for wound dressing, cell delivery in regenerative medicine,[3] drug delivery, and other biomedical applications in recent years.[4]

Naturally occurring polysaccharide chitosan (CS) have received much attention in biomaterial for its excellent biocompatibility.[5] However, its poor solubility in water and in common organic solvents restricts its wide spread utilization. The carboxymethylation of CS is a way for conversion of it into a water-soluble form. Carboxymethyl chitosan (CMCS) has many unique chemical, physical, and biological properties such as low toxicity, biocompatibility, and good ability to form films, fibers and hydrogels.[6,7] For this reason, it has been extensively used in many biomedical fields such as moisture-retention agent and bactericide in wound dressings, as artificial bone and skin in blood anticoagulants and as a component in the drug-delivery matrices.[8–10] Carboxymethyl cellulose (CMC) is the most widely used cellulose ether today, with applications in the detergent, food exploration, paper, textile, paint industries, and also in pharmaceutical.[11] Production of CMC is simpler than that of most other cellulose ethers because all reactions are operated at atmospheric pressure using commercially available reagents. The etherifying reagent, chloroacetic acid, is easy to handle and very efficient. For these reasons, CMC has become the largest industrial cellulose ether.

Applied Polymer SCIENCE

However, the hydrogels based on oxidized carboxymethyl cellulose (OCMC) blend with CMCS have never been reported. It would be interesting to study the preparation of OCMC-CMCS hydrogels by an easy method. This work aimed to prepare an OCMC-CMCS hydrogel with the purpose of creating new wound dressing materials. We examined the structure and swelling degree of the hydrogels. We also used a rat model to investigate the effect of the hydrogel on the epidermal wound healing in deep second degree burn.

EXPERIMENTAL

Materials

CS was purchased from Zhejiang Yuhuan Ocean Biochemistry (Zhejiang, China), and degree of deacetylation and molecular weight (M_w) were 90.2% and 2.1×10^5. Analytical grade CMC sodium salt was purchased from Fuchen Tianjing Chemical (Tianjing, China). All other chemicals were of reagent grade.

Carboxymethylation of Chitosan

Two reaction reagents, glyoxylic acid and chloroacetic acid, are currently used to prepare CMCS. Chloroacetic acid method was selected in this experiment.[12] CS was suspended in 50% NaOH solution. The mixture was kept at −20°C overnight. Isopropanol was then added into the frozen alkali CS as a reaction medium, followed by addition of chloroacetic acid. After stirring at room temperature for 30 min, heat was applied to bring the reaction mixture to the temperature of 30°C for another 6 h. The final products were dialyzed against deionized water for 3 days and then vacuum dried at 40°C.

Oxidation of Carboxymethyl Cellulose

Briefly, 10 g CMC was dispersed in 100 mL of ethanol. Different amounts of sodium periodate in 100 mL of water were then added and stirred. After stirring magnetically for 6 h in the dark at 30°C, the reaction was quenched by the addition of 2 mL of ethylene glycol and 3 g NaCl under stirring for 30 min. The final products were dialyzed against distilled water for 3 days and then vacuum dried at 40°C. When the molar ratios of sodium periodate to CMC were 0.3, 0.5, 0.7, and 0.9, OCMC with various degrees of oxidation were obtained. The degree of oxidation was estimated by determining the concentration of periodate left unconsumed by iodometry after 6 h. The degree of the oxidized products ranged from 30% to 60%. The solubility of OCMC was found to be increasing with increase in degree of oxidation.

Preparation of CMCS-OCMC Hydrogel

About 15 mL of CMCS (6% wt/vol aqueous solution) was mixed with 2, 5, and 8 mL OCMC (3% wt/vol aqueous solution), respectively. The mixture was allowed to stand for 10 min to get the CMCS-OCMC hydrogel (Scheme 1). As the volume ratios of OCMC to CMCS were 15/2, 15/5, and 15/8, the hydrogels were marked as CSOC-2, CSOC-5, and CSOC-8 accordingly.

Gelation Time

The gelation time test was performed according to the previously reported method.[13] A mixture of carboxymethyl chitosan (weight ratio = 6%) and oxidized carboxymethyl cellulose solution (weight ratio = 3%) was put on a petri-dish (100×20 mm^2, International VWR, Shanghai, China), and a magnetic stirring bar (Teflon fluorocarbon resin, 5×2 mm^2, Fisher Scientific, Shanghai, China) was placed in the center of the solution droplet. The solution was stirred at 155 rpm using a Corning model PC-320 hot plate/stirrer under UV illumination from a distance of 2 cm. Gelation time was noted as the time required for the stir bar to stop according to Yeo et al.[13] Values reported were average of 4–5 determinations ± standard deviation (SD).

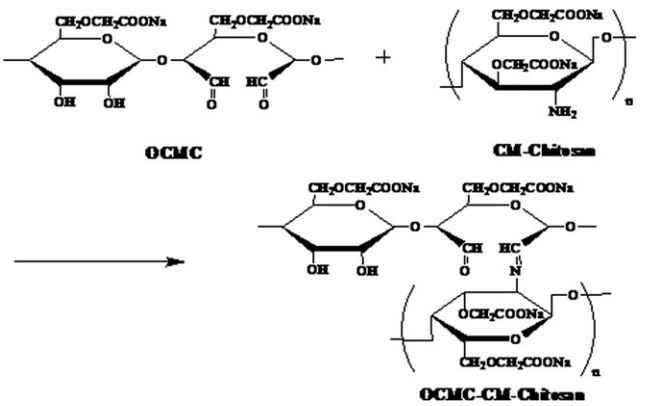

Scheme 1. Schematic illustration of the synthesis of crosslinked CMCS-OCMC hydrogel.

Swelling Degree Determination

The hydrogels were immersed in 5 mL phosphate buffered saline (PBS) solution at a pH of 3, 5, 7.4, 9, and 13 at 37°C for 24 h. The equilibrium fluid content, which represented the swelling degree of the hydrogel was calculated as follows:

$$\text{Equilibrium fluid content} = \frac{[W_s - W_d]}{W_s} \times 100\%,$$

where W_s is equilibrium weight of hydrogel in buffer saline and W_d is the absolutely dried weight of hydrogel. Each W_d determination contained no less than 0.1 g hydrogel, the average value of five samples was reported.[14] PBS solution, which readily provided different pH values required were prepared freshly. The standard PBS solution (pH = 7.4, 0.1M) was prepared by dissolving 17.97 g of di-sodium hydrogen phosphate, 5.73 g of monosodium hydrogen phosphate, and 9 g of sodium chloride in 1 L distilled water. The pH value was calculated as follows:

$$\text{pH} = \text{p}K_{a_2} - \log\frac{[\text{H}_2\text{PO}_4^-]}{[\text{HPO}_4^{2-}]} = 7.2 - \log\frac{[\text{H}_2\text{PO}_4^-]}{[\text{HPO}_4^{2-}]}.$$

Structural and Morphological Characterization

Fourier transform infrared spectra were recorded in a KBr disks using a Nicolet 170SX FTIR (Perkin–Elmer Co., Waltham, Massachusetts, USA) spectrometer equipped with Dynamic Ground Target Simulator detector and DMNIC 3.2 software over the range of 4000–400 cm^{-1}. For the morphological characterization, the CMCS-OCMC hydrogel membranes were analyzed with a scanning electron microscopy (SEM) (Hitachi S-570, Japan) with an acceleration voltage of 40 kV. The silica wafer was cleaned with the assistance of sonication in ethanol for 10 min, and then a thin layer of the sample was cast on it and freeze-

dried in a lyophilizer overnight. A layer of gold was spluttered on the sample by vacuum spray to make conduction surface.

In Vivo Wound Healing

The wound healing characteristics of the *in situ* formed hydrogel were evaluated using a rat model. All experiments were performed with the approval of the Animal Ethics Committee of the Third Hospital of Wuhan. The study animals were adult male Wistar rats (8 weeks old) each weighing approximately 220–250 g. The rats were purchased from shanghai laboratory animal center (Shanghai, China). Male Wistar rats weighing approximately 250 g were anesthetized by intramuscular injection of Ketamine and Xylaxin, at a dose of 40 and 5 mg/kg body weight, respectively. The skin of the animal was shaved and disinfected using 70% ethanol. And then the skin was exposed to water at 80°C for 8 s. The wound was photographed and the wound area was measured.[15]

Aqueous 6% CMCS solution and 3% OCMC solution were prepared and sterilized using steam autoclaving. About 1.5 mL of CMCS solution and 0.5 mL of OCMC solution, CSOC-5 hydrogel, were introduced onto the wound bed using the double syringe fibrin glue applicator. Spreading of the gel evenly on the wound bed was done immediately on application with the aid of fire-polished glass rod tip. The test wounds were then covered with sterile gauze, which was then fixed with elastic adhesive bandage. Similarly, control wounds also were covered with sterile gauze and elastic adhesive bandage without the test material. After the surgical procedure performed on a clean bench with an UV-C germicidal lamp, animals were kept in separate cages and fed with commercial rat feed and water *ad libitum* until they were sacrificed.

The rats were sacrificed by excess doses of sodium pentabarbitol on Day 3, 7, and 14 after surgery. The wounds were grossly examined and photographed for measurement of wound size reduction. For histology, the skin including the entire wound with adjacent normal skin was excised and fixed in 10% buffered formalin. The specimen included the dermis and the subcutaneous tissue. The wound size measurements taken at the time of surgery and at the time of biopsy were used to calculate the percent reduction in wound size using equation:

$$\text{Wound size reduction } (\%) = \frac{A_o - A_t}{A_o} \times 100,$$

where A_o and A_t are initial wound area and wound area after a time interval "t." Area was measured from the photographs of the wounds using the image analysis software (NIH Image tool III, MD).

Table I. Gelation Time of Crosslinked Carboxymethyl Chitosan-Oxidized Carboxymethyl Cellulose Hydrogel

Sample no.	The weight percent of OCMC/CMCS	Gelation time (s)
CSOC-2	6.7%	192
CSOC-5	12.5%	24
CSOC-8	20.0%	32

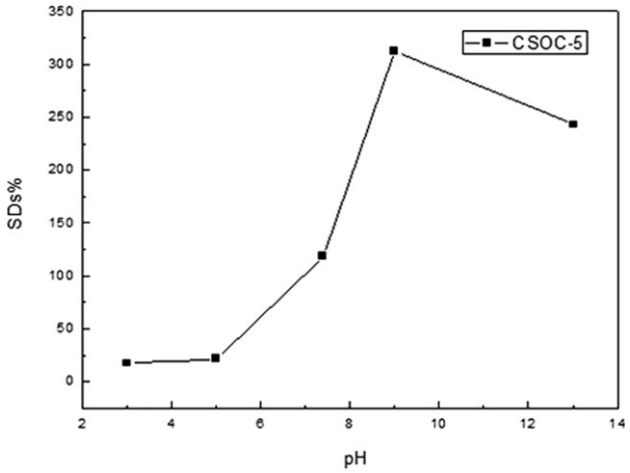

Figure 1. The equilibrium fluid content of CSOC-5 at different pH of phosphate buffer solution.

Histology

Excised wound sites fixed in formalin were processed and embedded in paraffin, and sections of 3–5 μm were stained with hematoxylin and eosin.

Statistical Analysis

Statistical analysis of data was performed by one way analysis of variance (ANOVA), assuming confidence level of 95% ($P < 0.05$) for statistical significance. All the data were expressed as mean ± standard deviation (SD).

RESULTS AND DISCUSSION

Gelation Time

Different amounts of OCMC were added to form different OCMC-CMCS hydrogels. The results of gelation time of the hydrogels are listed in Table I. As is shown, the hydrogels had the shortest gelation time of 24 s. Results indicated that the gelation time decreased at first when the weight percent of OCMC/CMCS increased from 6.7% to 12.5%, but as the weight percent of OCMC/CMCS increased from 12.5% to 20%, the

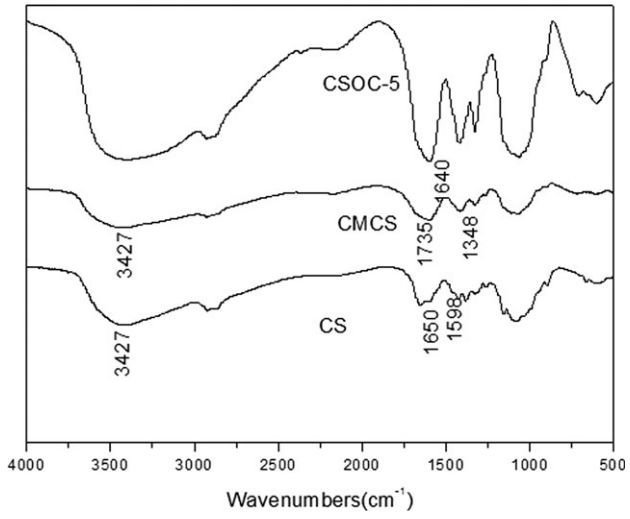

Figure 2. FTIR spectra of CS, CMCS, and CSOC-5.

Applied Polymer SCIENCE

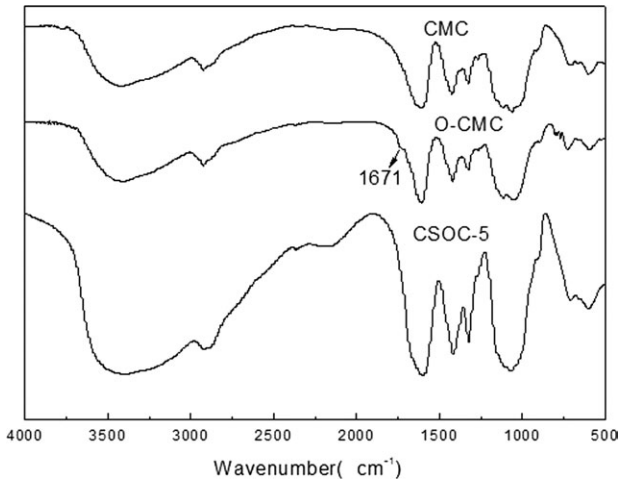

Figure 3. FTIR spectra of CMC, OCMC, and CSOC-5.

gelation time increased. As the amount of OCMC increased, the mixture provided more aldehyde groups to react with amino groups in CS which formed a crosslinked network structure, so that the gelation time decreased. Whereas when the weight percent of OCMC/CMCS was more than 12.5%, aldehyde groups in the solution became saturated. With the weight percent of OCMC/CMCS aqueous solution increasing, the concentration of the whole solution was reduced, which impeded aldehyde groups from reacting with amino groups to form the crosslinked network structure. This resulted in lower rates for hydrogel gelation.

Hydrogels Swelling Degree

The equilibrium fluid content of CSOC-5 at different pH of phosphate buffer solution is shown in Figure 1. The equilibrium fluid content, which represented the swelling degree of hydrogel, was studied. An obvious swelling behavior was observed for the hydrogel. The results revealed that the equilibrium fluid content was significantly influenced by pH, the equilibrium fluid content increased with the pH increasing from 3.0 to 9.0. The highest equilibrium fluid content of 312.83% could be observed under alkalic conditions (pH = 9.0) while the lowest equilibrium fluid content of 17.47% under acidic conditions (pH = 3.0). This could be attributed to the fact that at a low pH

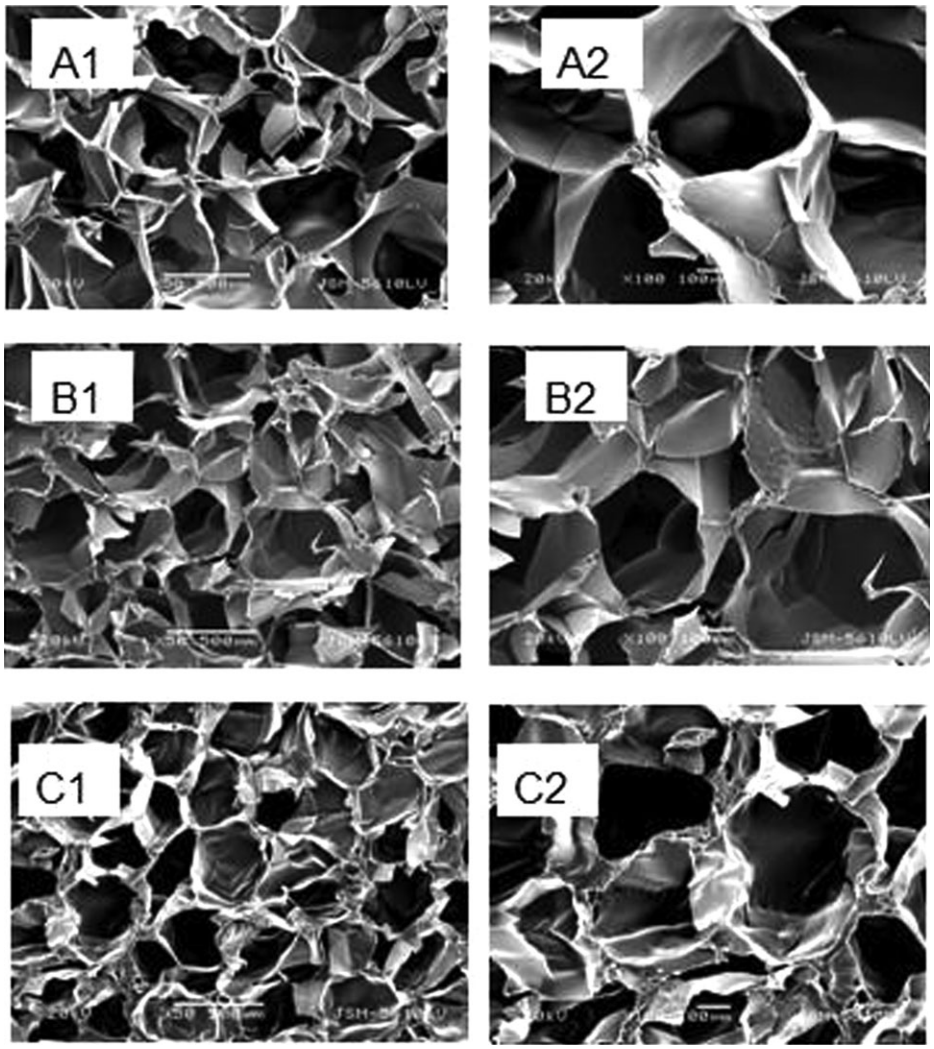

Figure 4. SEM images of CSOC-2 (A1 and A2), CSOC-5 (B1 and B2), and CSOC-8 (C1 and C2).

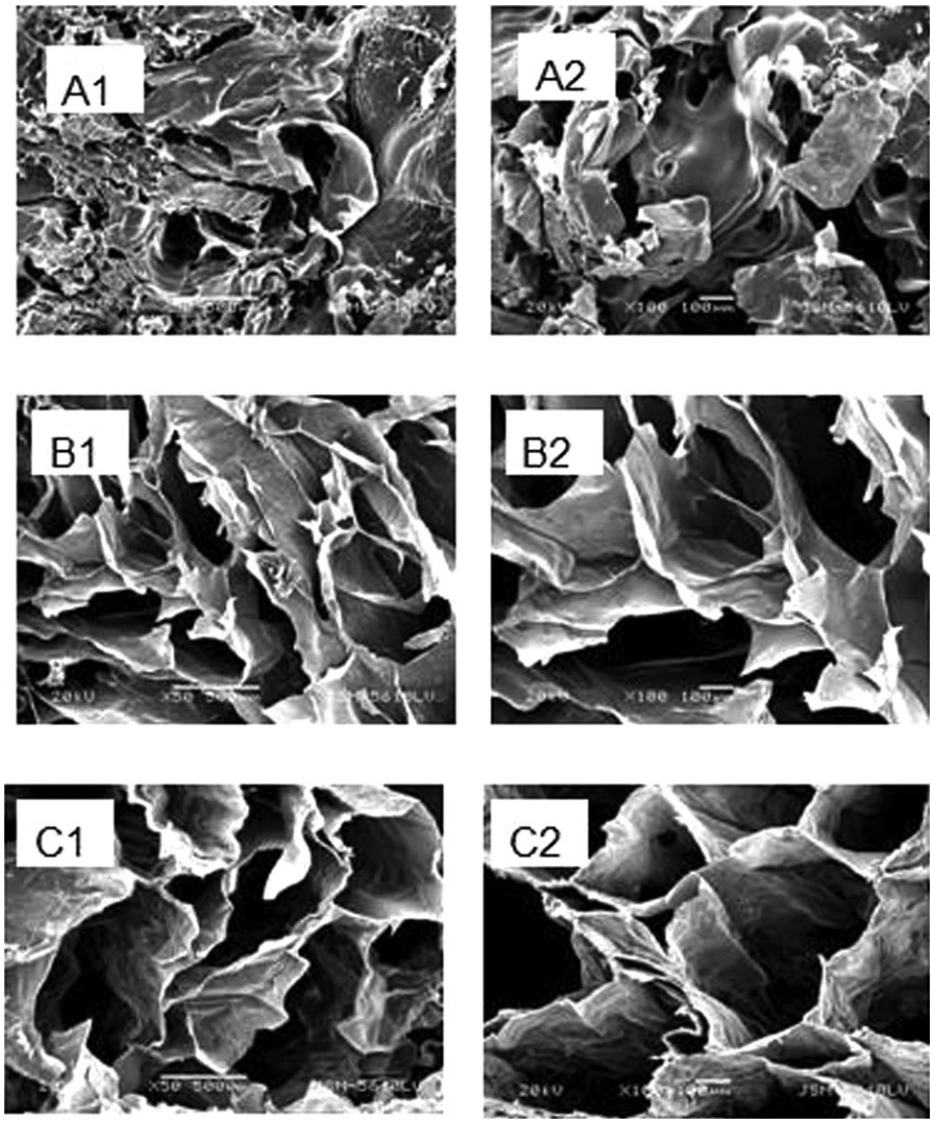

Figure 5. SEM images of CSOC-5 hydrogel in different buffer saline at different pH values: pH = 3.0 (A1 and A2), pH = 7.4 (B1 and B2), and pH = 13.0 (C1 and C2).

region, most carboxylic acid groups of CMCS and CMC are in the form of —COOH. As the pH of the medium increases, the carboxylic acid groups become ionized, and the resulting electrostatic repulsion caused the gels to swell. Moreover, at the pH ranging from 3.0 to 9.0, ionization of amino groups of CMCS took place, which could lead to the increase in the swelling ratio of CSOC hydrogel.[16]

Infrared Spectral Analysis of the Hydrogels

Figure 2 shows the infrared spectra of the CS, CMCS, and crosslinked CMCS-OCMC hydrogels (CSOC-5). From the infrared spectra of CS, we could see an absorption peak at 3427 cm^{-1}, which was due to the O—H stretching vibration, N—H extension vibration and the intermolecular H-bonds of the polysaccharide moieties. The peak at 1598 cm^{-1} was attributed to the deformation vibration of amino groups, and the one at 1650 cm^{-1} was assigned to amide stretching vibrations.[17] From the infrared spectra of CMCS, we could see a strong new peak at 1735 cm^{-1} representing the carboxylate C=O asymmetric stretching. The peak at 1384 cm^{-1} was assigned to the symmetric stretching vibration of carboxylate C=O. It demonstrated the successful introduction of the —COO group to CS chains. Compared with the infrared spectra of CS, the absorption peak of CMCS at about 3427 cm^{-1} became weak. It indicated that the O—H of CS had participated in the reaction (as the absorption peak at 3427 cm^{-1} was due to the O—H stretching vibration).

Compared with the infrared spectra of CMCS and crosslinked CMCS hydrogel (CSOC-5), it was found that a new absorption peak appeared at about 1640 cm^{-1}. It was the stretching vibration peak of —N=C—, which was produced by the Schiff's base reaction between amino groups in CMCS and aldehyde groups in OCMC. The occurrence of —N=C— structure proved that the crosslink reaction had taken place.

Applied Polymer SCIENCE

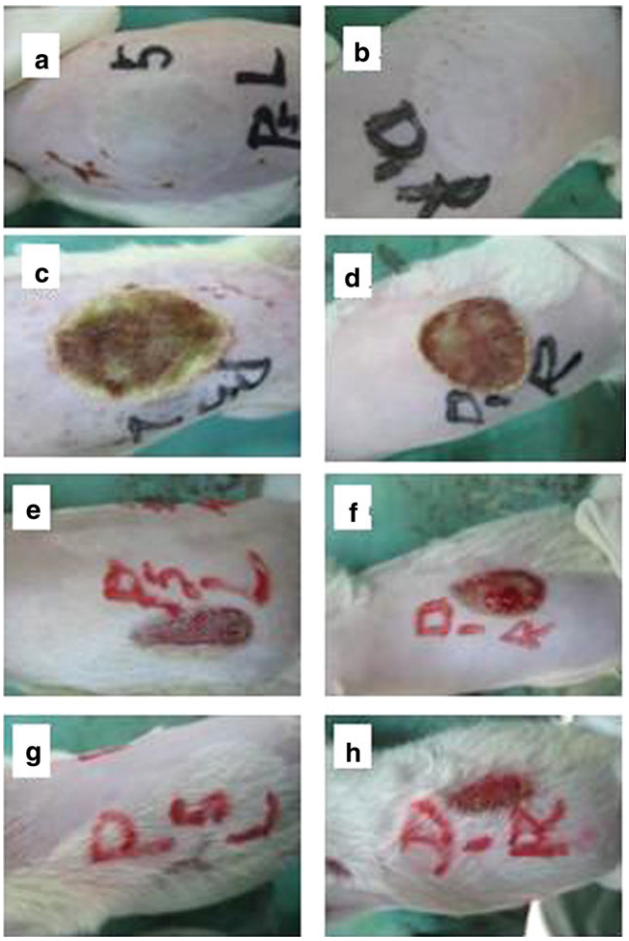

Figure 6. Representative photographs of macroscopic appearance of wounds excised on rat (a, b), test wounds of CSOC-5 hydrogel at 3 (c), 7 (e), and 14 days (g) and control wounds of normal saline at 3 (d), 7 (f), and 14 days (h). [Color figure can be viewed in the online issue, which is available at wileyonlinelibrary.com.]

Figure 3 presents the infrared spectra of the CMC, OCMC, and CMCS-OCMC hydrogel (CSOC-5). Compared with the infrared spectrum of CMC, OCMC had a new absorption peak at 1671 cm^{-1}, which could be attributed to the stretching vibration of —CHO,[16] proving that the oxidation reaction had taken place. The peak disappeared in the infrared spectra of hydrogel CSOC-5, which indicated the aldehyde groups of OCMC had been consumed in the crosslinking reaction.

Scanning Electron Microscopy

Figure 4 shows SEM photomicrographs of CMCS-OCMC hydrogel, displaying their morphology and internal space of the three-dimensional network structure. Figure 3(A–C) shows the morphology of CMCS-OCMC hydrogels with different amounts of OCMC (2, 5, and 8 mL, respectively) at different magnifications. From these electron micrographs, it could be observed that the crosslinked hydrogel formed a network structure in all concentrations used. And at the same magnification, the pore size of the hydrogels became smaller with the amount of OCMC solution increased. This was probably due to the fact that the more aldehyde groups OCMC provided, the more the degrees of crosslinking reacted with the amino groups of CMCS. Therefore, the structure of the hydrogels became more and more compact, and then the swelling degree decreased.

Figure 5 shows SEM micrographs of the hydrogels which have been immersed in buffer saline. Figure 4(A–C) represents the images of CMCS-OCMC hydrogels (with 15 mL CMCS aqueous solution and 5 mL OCMC aqueous solution) immersed in different buffer saline solutions at pH = 3.0, 7.4, and 13.0, respectively. A comparison between these images showed that the hydrogel in neutral and alkaline environments had a stable network structure. However, the pore size of these structures was not inerratic in acidic environment. It could be observed that the hydrogels in alkaline or neutral phosphate buffer solutions exhibited bigger pores in its internal spatial structure than in acidic phosphate buffer solution. The results indicated that the hydrogels swelled better in the alkaline or neutral conditions.

Gross Examination of Wound Healing

Grossly, each wound (both test group of CSOC-5 hydrogel and control group of normal saline) was observed for a period of 3, 7, and 14 days post-treatment (Figure 6). At 3 days, subcutaneous aspect appeared grossly normal for the test samples and there was no evidence of infection or contraction of the wound, while skin was hemorrhagic for some control samples and also scab was present on the wound bed. It has been reported that epithelialization is retarded by the dry scab. Winter showed that epithelialization can be accelerated if the wound is kept moist.[18] One explanation for this was that keratinocytes migrated more easily over a moist wound surface than underneath a dry one.[19] Epidermal cells can migrate at a speed of about 0.5 mm/day over a moist wound surface which is twice as fast as under a scab in dry wounds.[20] Subcutaneous aspects appeared grossly normal for test and control wounds at 7 days of post wounding and skin under the scab was hemorrhagic for both test and control samples. At Day 14, the majority of the test wounds appeared to be healed.

By measuring the wound area before and after definite intervals of time, reduction in wound defect area was calculated. At Day 3, there was no obvious reduction in wound defect area for both test and control. At Day 7, healing started leading to about 69.8% reduction in wound defect for test wounds, whereas for control wounds this value was about 65.8%. Statistical analyses revealed that this difference was not significant ($P > 0.05$). However, at Day 14, wound size reduction was of about 99.8% in the case of test wounds, whereas for control wounds this was about 79.9% which was statistically significant ($P < 0.05$).

Histological Examination

The healing pattern of wounds was studied by histological examination of the test and control samples (CSOC-5 hydrogel and normal saline) at 3, 7, and 14 days post-wounding.

In the dermis layers, severe inflammation was observed in both test and control wounds during this period [Figure 7(a, b)]. Inflammation is a normal and necessary prerequisite to healing.[21] Wound healing can be initiated by numerous causes,

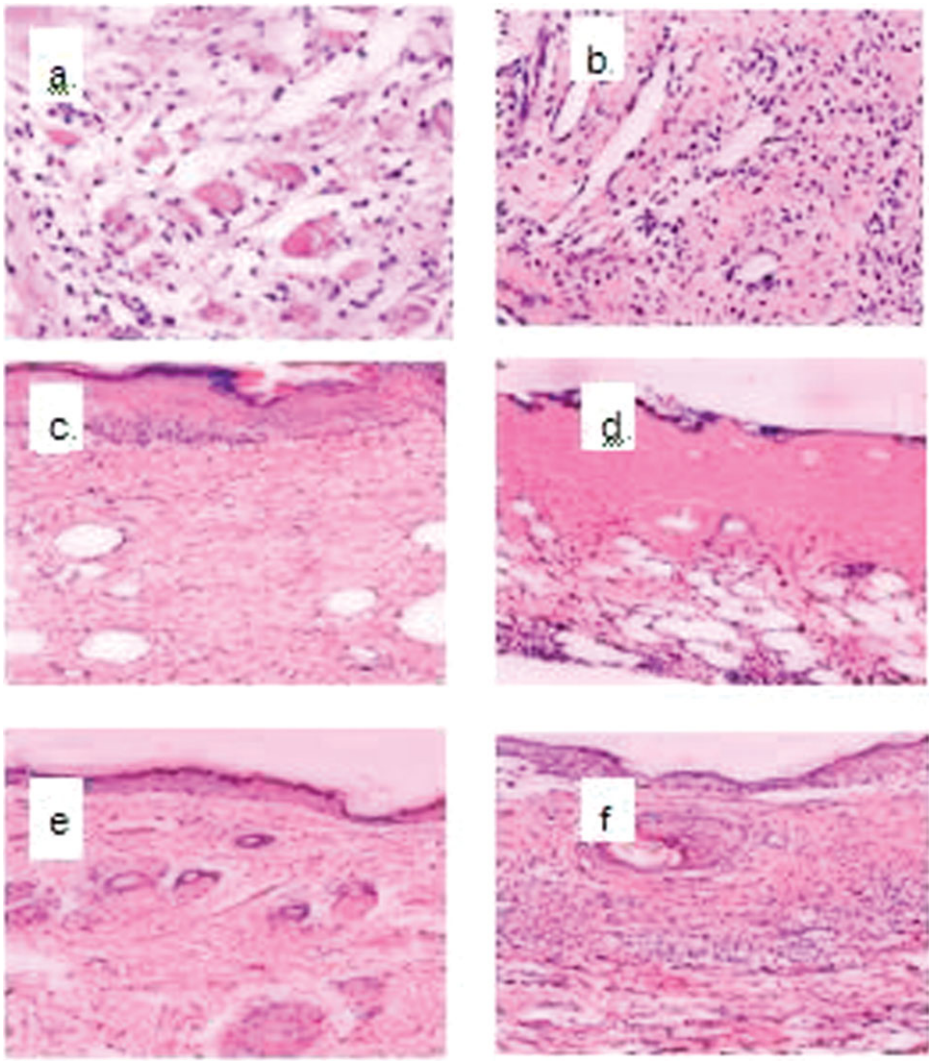

Figure 7. Histology of wound sections stained with hematoxylin and eosin. Test wound of CSOC-5 hydrogel (a, 400×) and control wound of normal saline (b, 300×) at Day 3; test wound of CSOC-5 hydrogel (c, 150×) and control wound of normal saline (d, 60×) at Day 7; test wound of CSOC-5 hydrogel (e, 100×), and control wound of normal saline (f, 100×) at Day 14. [Color figure can be viewed in the online issue, which is available at wileyonlinelibrary.com.]

one of which is injury. Therefore, during early stages of wound healing, it is difficult to assess whether the inflammatory response is part of normal healing process or due to the effect of material. No bacterial colony was found in any of the test or control wounds. Also, many new capillaries, which were of white mesh structures, were observed in the test group [Figure 7(a)] which was greater than that of control group [Figure 7(b)].

At Day 7, both test and control wounds appeared reduced in size with new epithelium noted at the edges of the defect [Figure 7(c, d)]. In test wounds [Figure7(c)], the defect area became filled with fibro-proliferative tissues, which were around outside the white blank, showing that they were in the process of healing. There were still some inflammatory cells in the dermis of the test wounds but much fewer than the test wounds at Day 3. Granulation tissue was observed in the dermis of both test and control wounds. Granulation tissue formation is essential for permanent wound closure, since it prepares the way for epithelialization and defect regeneration. These findings support that CMCS-OCMC hydrogel is able to provide suitable condition for granulation tissue formation.

At Day 14, in test wounds (7e), the defect area became smaller and the amount of inflammatory cells was considerably reduced. The surface of the defect was covered with new epithelium [Figure 7(e)]. However, for some control wounds although the surface of the defect was covered with new epithelium, a large number of inflammatory cells were still present in the dermis [Figure 7(f)]. In the present study, foreign body reaction subsided after 14 days demonstrating that the material was undergoing degradation on the wound bed and the degradation products were not inducing any adverse reaction within the body. However, the wound healing efficacy of the *in situ* forming hydrogel could be further improved by incorporating drugs or other growth factors.

CONCLUSIONS

In this work, *in situ* crosslinked hydrogels were obtained through the crosslinking reaction between OCMC and CMCS. Gelation time test showed that the hydrogels had the shortest gelation time of 24 s. The swelling degree was evaluated by determining the equilibrium fluid content. We found that the equilibrium fluid content was significantly influenced by pH. When the pH increased from 3.0 to 9.0, the equilibrium fluid content increased and the highest equilibrium fluid content reached 312.83% as pH = 9.0. The wound healing efficacy of hydrogel was evaluated and results indicated that the hydrogel was capable of providing suitable condition for granulation tissue formation without any adverse reaction within the body. This *in situ* forming hydrogel has potential to use as a wound dressing material in the wound management industry.

ACKNOWLEDGMENTS

The work was supported by the National Natural Science Foundation of China (Foundation No. 51173143, No. 50973088), Technology Innovation Foundation for SMEs of Ministry of Science of China (Foundation No. 11C26214202642, No. 11C26214212743), Supply and Demand Docking Program of Science and Technology of Wuhan (Foundation No. 201150124013), Wuhan Science and Technology Development (Foundation No. 201060623262), Key Research Project of Health Department of Hubei Province (Foundation No. JX4B54), Wuhan Academic Leaders Program (Foundation No. 200851430480), and Independent Innovation Research Foundation of Wuhan University of Technology (Foundation No. 2010-IV-070).

REFERENCES

1. Drury, J. L.; Mooney, D. *J. Biomaterials* **2003**, *24*, 4337.
2. Varghese, S. Hwang, N. S.; Canver, A. C.; Theprungsirikul, P.; Lin, D. W.; Elisseeff, J. *Matrix Biol.* **2008**, *27*, 12.
3. Thierry, D. *Carbohydr. Polym.* **2012**, *87*, 1013.
4. Yin, W.; Su, R.; Qi, W. *J. Mater. Sci.* **2012**, *47*, 2045.
5. Xu, Y. M.; Zhan, C. Y.; Fan, L. H.; Wang, L.; Zheng, H. *Int. J. Pharm.* **2007**, *336*, 329.
6. Muzzarelli, R. A. A. *Carbohydr. Polym.* **1988**, *8*, 1.
7. Chen, L.; Du, Y.; Tian, Z.; Sun, L. *J. Appl. Polym. Sci.* **2005**, *43*, 296.
8. Liu, Z.; Jiao, Y.; Zhang, Z. *J. Appl. Polym. Sci.* **2007**, *103*, 3164.
9. Janvikul, W.; Thavornyutikarn, B. *J. Appl. Polym. Sci.* **2003**, *90*, 4016.
10. Muzzarelli, R. A.; Ramos, V.; Stanic, V.; Dubini, B. *Carbohydr. Polym.* **1998**, *36*, 267.
11. Methacanon, P.; Chaikumpollert, O.; Thavorniti, P.; Suchiva, K. *Carbohydr. Polym.* **2003**, *54*, 335.
12. Muzzarelli, R. A. A. *Carbohydr. Res.* **1982**, *107*, 199.
13. Yeo, Y.; Geng, W. L.; Ito, T. C. *J. Biomed. Mater. Res.* **2007**, *81*, 312.
14. Andreopoulos, F. M.; Indushekhar, P. *Biomaterials* **2006**, *27*, 2468.
15. Balakrishnan, B.; Mohanty, M.; Umashankar, P. R.; Jayakrishnan, A. *Biomaterials* **2005**, *26*, 6335.
16. Gao, C. M.; Liu, M. Z.; Chen, S. L.; Jin, S. P.; Chen, J. *Int. J. Pharm.* **2009**, *371*, 16.
17. El-Sherbiny, I. M. *Eur. Polym. J.* **2009**, *45*, 199.
18. Winter, G. D. *Nature* **1962**, *193*, 293.
19. Winter, G. D. Scales, J. T. *Nature* **1963**, *197*, 91.
20. Winter, G. D. In Epidermal Wound Healing; Maibach, H. I., Rovee, D. T., Eds.; Yearbook Medical Publishers, Inc.: Chicago, **1972**; p 71.
21. Kirsner, R. S.; Eaglstein, W. H. *Am. J. Clin. Dermatol.* **1993**, *11*, 629.